Measurement of Cross-Field Heat Transport in a Nonneutral Plasma

E. M. Hollmann, F. Anderegg, and C. F. Driscoll

Institute for Pure and Applied Physical Sciences,
University of California at San Diego, La Jolla, CA 92093-0319, USA

Abstract. The cross-magnetic field heat transport in a Mg^+ plasma confined in a Penning-Malmberg trap is found to be dominated by novel long-range collisions. The measurement uses two lasers: a strong cooling beam creates a controlled temperature gradient in the plasma and a weak probe beam measures the ion temperature evolution. The temperature gradient drives a heat flux which dominates the measured temperature evolution, with corrections due to small external heating terms. Classical theory of collisional heat conductivity considers only ion-ion collisions with collisionality ν and impact parameter $\rho < r_c$, giving thermal diffusivity $\chi_c \propto \nu r_c^2$. Here, long-range collisions with impact parameter $r_c < \rho < \lambda_D$ can dominate the heat transport, giving $\chi_L \simeq \frac{1}{2}\nu\lambda_D^2$. Initial measurements taken for a plasma with temperature $T \simeq .02$ eV and density $n \simeq 5 \times 10^7 cm^{-3}$ at B = 4 T show enhanced heat transport consistent with thermal diffusion dominated by these long-range collisions.

I INTRODUCTION

The study of heat transport in plasmas is an area of extensive research in astrophysics [1], laser physics [2], plasma processing [3], and especially in magnetic fusion research [4]. Quiescent plasmas with a single sign of charge (nonneutral plasmas) are, because of their superior stability and confinement properties, important for basic plasma physics and atomic physics research [5,6]. These properties also make nonneutral plasmas ideal systems for the study of collisional heat transport.

Heat can be transported across the magnetic field from both short-range and long-range collisions. The standard "classical" theory of heat flow across a magnetic field was derived for neutral plasmas in the regime $r_c > \lambda_D$, where $\lambda_D \equiv \sqrt{\frac{kT}{4\pi ne^2}}$ is the Debye shielding length and $r_c \equiv \frac{\bar{v}}{\Omega_c} = \frac{\sqrt{kT/m}}{eB/mc}$ is the cyclotron radius. The resulting thermal diffusivity is given by $\chi_c = \frac{16}{15}\sqrt{\pi}\ln(r_c/b)\nu r_c^2$, where $\nu \equiv n\bar{v}b^2$ is the collisionality and $b \equiv \frac{e^2}{kT}$ is the classical distance of closest approach [7]. Here, the basic transport mechanism is velocity- scattering collisions with impact parameter $\rho \leq r_c$, so that heat is transported across the magnetic field by particles taking cyclotron radius-sized steps. Nonneutral plasma experiments typically operate in the regime $\lambda_D \gg r_c$ because of the Brillouin density limit [8] . In this regime, calculations predict that the thermal diffusivity is dominated by "long-range" collisions, giving thermal diffusivity $\chi_L \simeq 0.49\nu\lambda_D^2$ [9]. Here, the particles feel each others' electric fields on the scale of λ_D and the basic transport mechanism is the tranfer of parallel velocities over distances of order λ_D. The perpendicular velocities of the particles remain fairly constant during these long-range collisions, and the interacting particles remain well-separated in space. There is a slight cross-field drift due to these collisions, which is negligible for the purposes of heat transport calculations, but is important for particle and angular momentum transport [10].

Here, we present heat transport measurements which support the presence of long-range collisional transport. Data is presented for a nonneutral Mg^+ plasma with B = 4 T, $n \simeq 5 \times 10^7 cm^{-3}$, and $T \simeq .02$ eV. The corresponding equipartition rate, $\nu_{\perp\parallel} \equiv \frac{8}{15}\sqrt{\pi}\ln(r_c/b)\nu \simeq 400/s$, is large, so that the temperatures parallel and perpendicular to the magnetic field are well-equilibrated, i.e. $T_\parallel = T_\perp = T$. For diffusive heat transport, the local heat flux Γ_q is proportional to the local plasma density n, thermal diffusivity χ, and temperature gradient ∇T:

CP457, *Trapped Charged Particles and Fundamental Physics*
edited by Daniel H. E. Dubin and Dieter Schneider

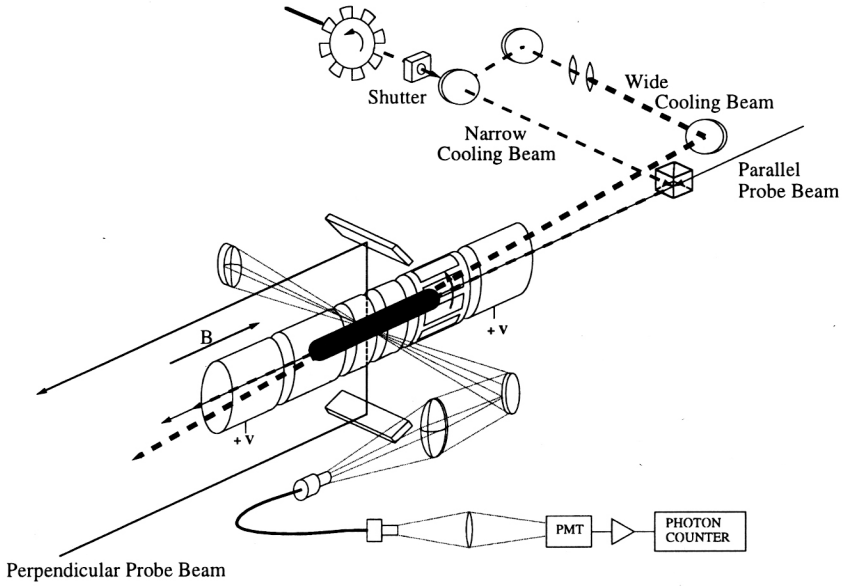

FIGURE 1. Ion trap schematic showing cooling beam and probe beam geometries.

$$\Gamma_q = -\frac{5}{2} n \chi \nabla \mathrm{T} \ . \tag{1}$$

The local energy density, $q \equiv \frac{3}{2} n \mathrm{T}$, changes at a rate related to the heat flux by conservation of energy:

$$\dot{q} = -\nabla \cdot \Gamma_q + \dot{q}_{ext} \ . \tag{2}$$

Here, $\dot{q}_{ext}$ represents the local sum of external heat sinks and/or sources acting on the plasma. We believe $\dot{q}_{ext}$ to be dominated by collisions with the background gas and by Joule heating due to the slow radial expansion of the ion cloud. We measure $\dot{q}_{ext}$ by creating an initial condition with $\nabla \mathrm{T} \simeq 0$, so that the measured heating rate at each point in space is dominated by the external heating term, i.e. $\dot{q} \simeq \dot{q}_{ext}$. For the data presented here, the density n evolves on a time scale which is slow ($\sim$ 1000 sec) compared to the time scale on which the temperature T evolves ($\sim$ 1 sec), so that $\dot{q} \simeq \frac{3}{2} n \dot{\mathrm{T}}$.

II EXPERIMENTAL SETUP

Figure 1 shows the experimental setup used. The magnesium ions are created with a metal vacuum vapor arc (MEVVA) [11] and are trapped in a Penning-Malmberg trap with uniform axial magnetic field B = 4 Tesla and end-confinement potentials of 200 V. For the data presented here, 5×10^8 Mg^+ ions are confined in a plasma cylinder with length $L_p \simeq 14$ cm, radius $R_p \simeq 0.5$ cm, and density $n \simeq 5 \times 10^7 \mathrm{cm}^{-3}$. The radial electric field from the ion space charge causes the plasma column to $\mathbf{E} \times \mathbf{B}$ rotate at a frequency of $f_E \simeq 18$ kHz. This rotation is rapid compared to the transport time scales discussed here, so the radial, cross-field transport measurements are azimuthally-averaged. The conducting electrodes used in the trap have a wall radius $R_w = 2.86$ cm. The trap operates with a neutral background pressure of $P_N \simeq 4 \times 10^{-9}$ Torr of H_2.

The ion plasma is held in a steady, near-thermal equilibrium state by a "rotating wall" field applied using a sectored ring at one end of the plasma. The rotating wall torques on the plasma and balances the background drags due to neutrals and trap asymmetries, thus allowing steady-state plasma confinement [12]. Here, the applied field is turned off during the heat transport experiment; however, we find that the results obtained for the thermal diffusivity in this plasma are the same with or without the rotating wall applied.

Heat transport experiments are performed using two continuous 280 nm laser beams: a weak ($\simeq 10$ μW) probe beam is used to nonperturbatively measure the plasma density and temperature, while a stronger ($\simeq 1$ mW) cooling beam is used to cool the plasma. Normally, the plasma relaxes to an equilibrium temperature T $\simeq .05$ eV, determined by the balance between cooling from neutral collisions and heating due to the

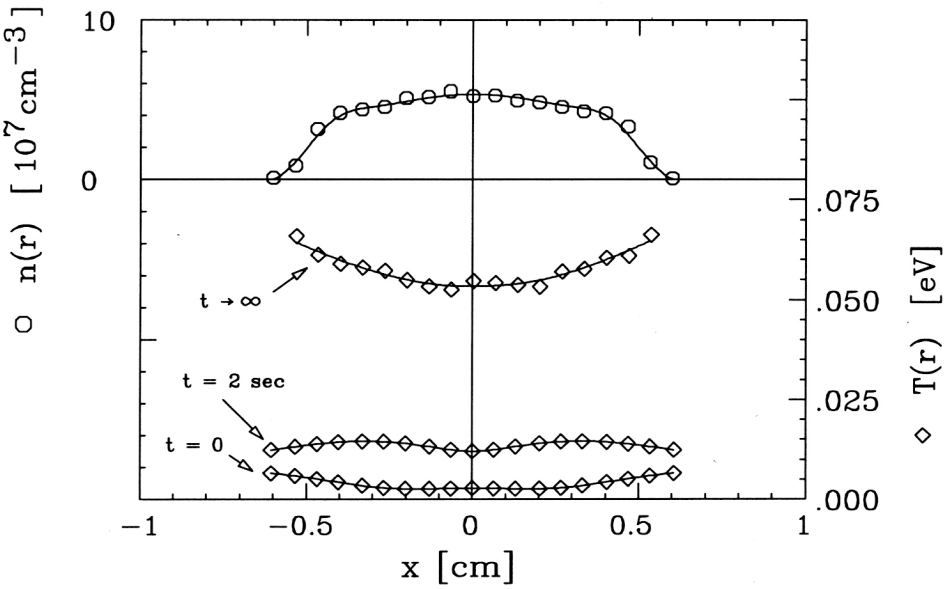

FIGURE 2. Measured plasma heating starting from uniformly cooled initial condition.

slow plasma expansion or due to the rotating wall drive. By detuning the cooling beam slightly off-resonance (- 2 GHz) from the cyclic $3^2S_{1/2} \rightarrow 3^2P_{3/2}$ Mg^+ transition, the plasma equilibrium temperature is cooled to about 3×10^{-3} eV. This laser cooling can be localized to the center of the plasma cylinder ($r \simeq 0$) by shining the cooling beam along the plasma axis, or made uniform over the whole plasma by widening the beam and shining it at an angle through the column.

The plasma density and temperature evolution, $n(r,t)$ and $T(r,t)$, are measured using the probe beam. The probe beam is scanned in frequency through the cyclic transition at each radial position, and the resulting Doppler-broadened scattered photon signal, $f(v, r, t = 0)$, is fit to three shifted Maxwellians (one for each Mg isotope) to obtain $n(r, t = 0), T(r, t = 0)$ [11]. The probe beam can be used to measure the temperatures both parallel and perpendicular to the magnetic field: for the data presented here, we find the temperatures to be well-equilibrated. The cooling beam is chopped at 50 Hz and the photon counting is performed synchronously with the chopper, so that only scattered light from the probe beam is measured. At t = 0, the cooling beam is blocked with a shutter so that the plasma temperature profile relaxes toward its normal equilibrium value, $T(r, t \rightarrow \infty) \simeq .05$ eV. Here, since the temperature evolution is much faster than the density evolution, i.e. $n(r,t) \simeq n(r, t = 0)$, we can measure the rapid temperature evolution by recording the peak of the scattered signal, $f(v = 0, r, t)$. Repeating experiment at different radii, r, gives the temperature evolution of the entire radial profile, $T(r, t)$.

III MEASUREMENT OF BACKGROUND HEATING TERMS

Measurement of the background heating terms, $\dot{q}_{ext}$, is performed by using the wide cooling beam so that the plasma is cooled uniformly. After the plasma has reached a uniformly-cooled equilibrium, the cooling beam is turned off. The subsequent measured time evolution of the plasma, $T(r, t)$, gives $\dot{q}_{ext}$ through Equations (1) and (2) since $\nabla T \simeq 0$. Figure 2 shows the result of this experiment: at $t = 0$, the plasma is cooled uniformly to $T(r, t = 0) \simeq 3 \times 10^{-3}$ eV. When the cooling beam is turned off, the plasma is observed to heat toward $T(r, t \rightarrow \infty) \simeq .05$ eV. For clarity, only T(r,t = 0) and T(r,t = 2 sec) are shown; actually 100 time steps ($t = 0$ to $t = 4$ sec) are measured at each radial position.

From the data shown in Figure 2, we obtain an external heating rate which agrees reasonably well with the calculated values for this plasma assuming Joule heating from the plasma expansion plus heating due to collisions with the room-temperature background gas. The Joule heating contribution is estimated by performing an independent experiment to measure the slow density evolution of this plasma, $n(r, t)$, when the rotating wall is turned off. This gives the bulk radial particle flux, Γ_b, from particle conservation: $\partial n/\partial t + \nabla \cdot \Gamma_b = 0$. We find $\Gamma_b \simeq 10^4$ cm^{-2}s$^{-1}(n/10^7$cm$^{-3})(r/1$cm), which gives an estimated Joule heating near

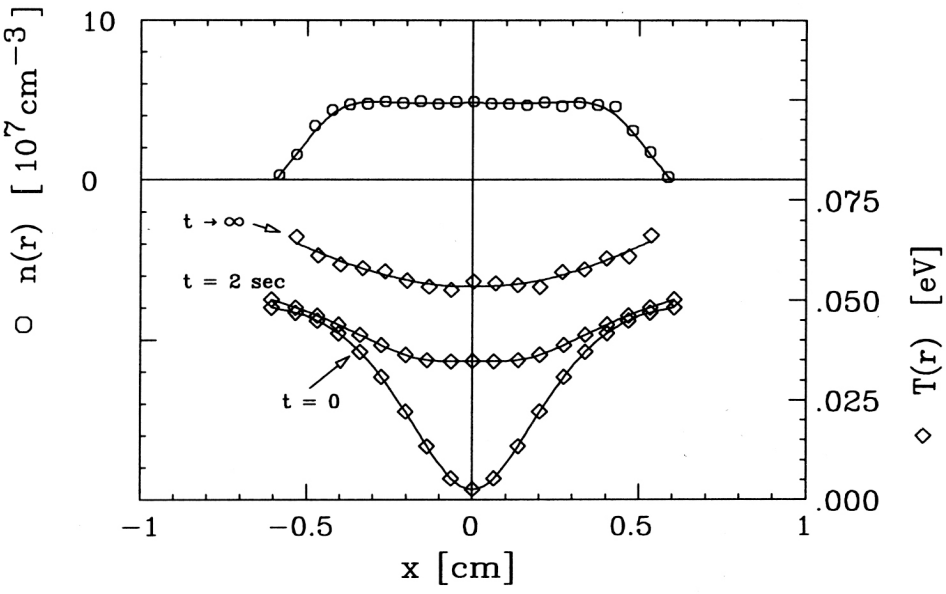

FIGURE 3. Measured thermal diffusion starting from locally (r=0) cooled initial condition.

$r = 0$ of $\dot{q}_J = env_r E_r = \frac{eB}{c}\omega_E r\Gamma_b \simeq 1.8 \times 10^5 \frac{\text{eV}}{\text{cm}^3\text{s}}\rho^2$, with $\rho \equiv (r/0.3\,\text{cm})$. To estimate the heating rate due to the collisions with the neutral gas, we use $\dot{q}_N = \frac{3}{2}n\dot{\text{T}} \simeq -\frac{3}{2}n\sigma n_N u(\text{T} - \text{T}_N)$, where u is the average relative particle velocity and T_N is the effective neutral gas temperature as seen by the rotating plasma: $\text{T}_N \simeq .024$ eV $[1 + .4\rho]$. To estimate the collision cross-section, σ, we use the Langevin cross-section [13], $\sigma = 2\pi\frac{e}{u}\sqrt{\alpha/\mu}$, where $\alpha \simeq 5\,a_0^3$ is the polarizability of H_2 and μ is the reduced mass. This gives a neutral heating rate $\dot{q}_N \simeq 2.8 \times 10^5 \frac{\text{eV}}{\text{cm}^3\text{s}}$ $[1 + .4\rho]$ and a total predicted heating rate $\dot{q}_{ext} = \dot{q}_J + \dot{q}_N \simeq 2.8 \times 10^5 \frac{\text{eV}}{\text{cm}^3\text{s}}$ $\left[1 + .4\rho + .6\rho^2\right]$. This agrees reasonably well with the measured heating of Figure 2 between $t = 0$ and $t = 2$ seconds: $\dot{q}_{ext} \simeq 3.7 \times 10^5 \frac{\text{eV}}{\text{cm}^3\text{s}}[1 + .1\rho]$.

IV MEASUREMENT OF THE HEAT FLUX

The heat flux experiment is shown in Figure 3. Here, the plasma is cooled locally at $r = 0$, creating an initial condition with a strong temperature gradient with a central temperature $\text{T}(r = 0, t = 0) \simeq 3 \times 10^{-3}$ eV. When the cooling beam is turned off, the plasma temperature is observed to rise rapidly toward the equilibrium temperature of $\text{T}(r, t \to \infty) \simeq .05$ eV. As in Figure 2, we show only time steps $t = 0$ and $t = 2$ sec for clarity. It can be seen, however, that the central temperature rises more rapidly than is observed in the experiment with no temperature gradient (Figure 2). At early times ($t = .1$ sec), the measured rate of change of the central temperature is found to be about 10× larger than for the data with no temperature gradient. Thus, we have a clear signal of heat flowing radially inward from the edges of the plasma.

The radial heat flux, Γ_q, is obtained from the measured $\text{T}(r, t)$ using Equation (2) and the measured $\dot{q}_{ext}(r)$. The best signal-to-noise for Γ_q was obtained at radii $r \simeq 0.1 \to 0.2$ cm. Figure 4 shows the heat flux measured at radii $r = 0.1 \to 0.2$ cm and at times $t = .1 \to 1.9$ sec. Over this range of r and t, the density remains fairly constant, $n \simeq 5 \times 10^7 \text{cm}^{-3}$, but the temperature varies by about a factor of four: $T \simeq .01 \to .04$ eV. Because of this, we divide the displayed Γ_q by the expected temperature scaling of the thermal diffusivity, $\chi \propto \text{T}^{-1/2}$.

The data in Figure 4 indicates that the heat flux is diffusive in nature and is in reasonable agreement with the predictions of the long-range collisional theory. From the straight (solid) line fit through the data, it can be seen that our model $\Gamma_q \propto \text{T}^{-1/2}\nabla\text{T}$ describes the data well. Both classical and long-range collisions predict a heat flux which satisfies this scaling. However, as can be seen from the theory predictions for this plasma (dashed lines), the magnitude of the measured heat flux is about 8× too large to be described by classical, short-range collisions alone, but is within reasonable agreement (about 80%) of the predictions of short-range plus long-range collisions.

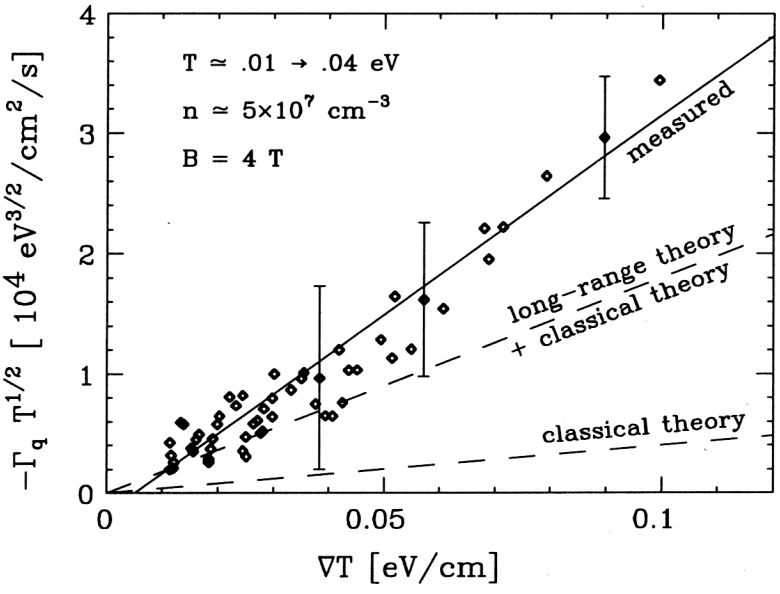

FIGURE 4. Measured radial heat flux vs. temperature gradient. The heat flux is multiplied by the measured $T^{1/2}$ at each point to remove the expected temperature scaling of the thermal diffusivity. Solid line fit passes through data and origin, indicating diffusive heat flux. Fit is is within 80% of long-range theory + classical theory, but 8× larger than classical theory alone.

This preliminary measurement provides evidence that the thermal diffusivity in nonneutral plasmas is dominated by long-range collisions with impact parameter of order of a Debye length; the standard thermal diffusivity based on collisions with impact parameter of order the cyclotron radius can therefore usually be neglected for these plasmas. For very large and/or strongly correlated nonneutral plasmas ($R_p > 100\,\lambda_D$ and/or $\Gamma > 1$), the heat conduction is predicted to be dominated by wave (nondiffusive) transfer of energy. Future experiments will attempt to test these predictions.

We gratefully acknowledge the support of the Office of Naval Research (ONR N00014-96-1-0239) and the National Science Foundation (NSF PHY94-21318).

REFERENCES

1. S. M. Ichimaru, H. Iyetomi, and S. Tanaka, Phys. Rep. **149**, 93 (1987); S. Pistinner, A. Levinson, and E. Eichler, Astrophys. J. **467**, 162 (1996).
2. T. Ditmire, E. T. Gumbrell, R. A. Smith, A. Djaoui, and M. H. R. Hutchinson, Phys. Rev. Lett. **80**, 720 (1998).
3. M. Tuszewski, Phys. Plasmas **5**, 1198 (1998).
4. F. Wagner and U. Stroth, Plasma Phys. and Contr. Fusion **35**, 1321 (1993).
5. T. M. O'Neil, in *Non-neutral Plasma Physics*, edited by G. M. Bunce, AIP Conf. Proc. No. 175 (AIP, New York, 1988), 1.
6. J. N. Tan, J. J. Bollinger, and D. J. Wineland, IEEE Trans. Instrum. Meas. **44**, 144 (1995).
7. M. N. Rosenbluth and A. N. Kaufmann, Phys. Rev. **109**, 1 (1958).
8. L. Brillouin, Phys. Rev. **67**, 260 (1945); R. C. Davidson, *Physics of Nonneutral Plasmas* (Addison-Wesley, Redwood City, 1989) p. 42.
9. D. H. E. Dubin and T. M. O'Neil, Phys. Rev. Lett. **78**, 3868 (1997).
10. D. H. Dubin, Phys. Plasmas **5**, 1688 (1998).
11. F. Anderegg, X. -P. Huang, E. Sarid, and C. F. Driscoll, Rev. Sci. Instrum. **68**, 2367 (1997).
12. X. -P. Huang, F. Anderegg, E. M. Hollmann, C. F. Driscoll, and T. M. O'Neil, Phys. Rev. Lett. **78**, 875 (1997); "Rotating Field Confinement of Pure Electron Plasmas Using Trivelpiece-Gould Modes", F. Anderegg, E. M. Hollmann, and C. F. Driscoll, submitted to Phys. Rev. Lett.
13. P. Langevin, Ann. Chim. Phys. **8**, 245 (1905).